Acta Cryst. (1996). B52, 432–439

Cation Disorder in Ferroelectric $PbBi_2Nb_2O_9$

V. SRIKANTH,[a] H. IDINK,[a] W. B. WHITE,[a]* E. C. SUBBARAO,[a]† H. RAJAGOPAL[b] AND A. SEQUEIRA[b]

[a]*Materials Research Laboratory, The Pennsylvania State University, University Park, PA 16802 4800, USA, and* [b]*Bhabha Atomic Research Centre, Bombay 400085, India*

(*Received 18 February 1993; accepted 1 November 1995*)

Abstract

The ferroelectric Curie temperature, T_c, of $PbBi_2Nb_2O_9$ was found to shift from 833 K in samples slowly cooled from 1373 K to T_c's up to 883 K when the samples were quenched from various temperatures in the range 973–1373 K. The variation of T_c with heat treatment was fully reversible. Extra Raman modes appear and the width of some Raman bands change as a function of heat treatment. These results are interpreted in terms of cation order–disorder involving the Pb^{2+} and Bi^{3+} ions in the perovskite units and the Bi_2O_2 layer. Neutron Rietveld analyses of the structures (orthorhombic, $A2_1am$, $Z = 4$, $\lambda = 1.216$) indicate a possible change in cationic order–disorder, with Pb^{2+} ions preferentially occupying the perovskite *A*-sites to the extent of 91 (7) and 80 (7)%, respectively, in the quenched and slowly cooled samples.

1. Introduction

Lead bismuth niobate, $PbBi_2Nb_2O_9$ is an Aurivillius-type compound (Aurivillius, 1949, 1950, 1952) in which perovskite-like $(PbNb_2O_7)^{2-}$ units (two ABO_3 units) are sandwiched between two $(Bi_2O_2)^{2+}$ layers along a pseudotetragonal *c* axis (Fig. 1). Although no re-examination of the crystal structure of $PbBi_2Nb_2O_9$ seems to have been undertaken since the early work of Aurivillius, the crystal structures of related compounds such as Bi_3TiNbO_9 (Wolfe, Newnham, Smith & Kay, 1971; Thompson, Rae, Withers & Craig, 1991), $(Sr,Ba)Bi_2Ta_2O_9$ (Newnham, Wolfe, Horsey, Diaz-Colon & Kay, 1973) and $SrBi_2Ta_2O_9$ (Rae, Thompson & Withers, 1992) have been examined in detail. The room-temperature orthorhombic ferroelectric form transforms to a tetragonal paraelectric phase at a Curie temperature around 833 K (Smolenskii, Isupov & Agranoskaya, 1961). In a comprehensive study of ferroelectricity in layer compounds of the Aurivillius type, Subbarao (1962*a*,*b*) observed that the Curie temperature of $PbBi_2Nb_2O_9$ appeared to depend on the heat treatment of the ceramic sample and he postulated that this behavior may be due to disorder in the distribution of the Pb^{2+} and Bi^{3+} ions in the two types of cation sites. The present study was undertaken to determine systematically the shift in Curie temperature with heat treatment, as shown in the permittivity–temperature data, and to seek support for cation disorder *via* a detailed study of the Raman spectra as a function of heat treatment of $PbBi_2Nb_2O_9$ ceramics. The interpretation of the dielectric and spectroscopic data was confirmed by a neutron diffraction study of a quenched and a slow-cooled sample.

It may be noted that while X-ray diffraction cannot provide useful information on cation disorder in this compound, neutron diffraction could provide only limited information as the neutron scattering lengths of Pb and Bi differ by ~10% only. Hence the use of Raman spectroscopy. Further, there does not seem to be any earlier Raman study of this compound, although the systematic Raman spectra of many Aurivillius phases have been published recently (Graves, Hua, Myhra & Thompson, 1995).

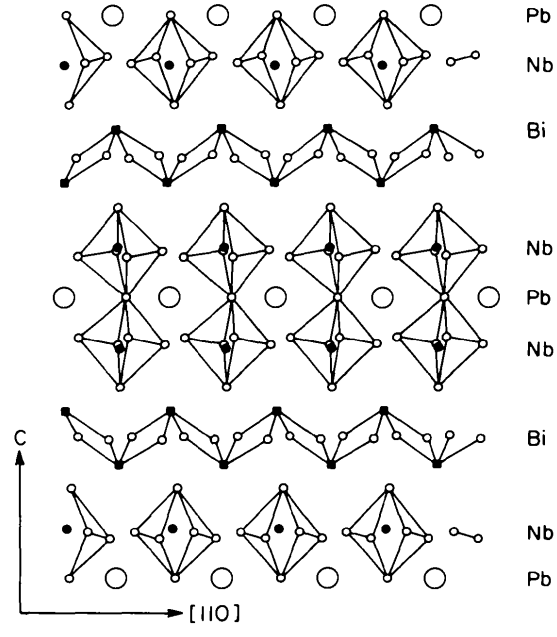

Fig. 1. Crystal structure of $PbBi_2Nb_2O_9$ showing the relation of perovskite layers and bismuth oxide layers.

† Permanent address: Tata Research, Development and Design Centre, 1 Mangaldas Road, Pune 411050, India.

An interesting observation has been reported regarding the dielectric behavior of a related compound, $BaBi_2Nb_2O_9$. Early dielectric measurements on $BaBi_2Nb_2O_9$ ceramics indicated a phase transition at ~483 K (Subbarao, 1962*a*). However, more careful measurements showed the temperature corresponding to the dielectric constant peak was dependent on frequency (Newnham, Wolfe & Dorrian, 1971), suggestive of relaxor-type behavior. Further, the measurements on single crystals of $BaBi_2Nb_2O_9$ did not show any evidence for a phase transition above room temperature (Newnham *et al.*, 1971).

2. Experimental

2.1. *Sample preparation*

Stoichiometric amounts of the oxides PbO, Bi_2O_3 and Nb_2O_5 were mixed in ethyl alcohol for 24 h. After drying and calcination at 1273 K, 2% polyvinyl alcohol was added and pellets ~1 cm in diameter were pressed. Sintering was carried out at 1373 K for 8 h, after which the pellets were cooled at a rate of 5 K min^{-1}. The density of the sintered pellets was 6.562 g cm^{-3}.

A number of pellets were heated in the furnace to 1373 K. After holding them at 1373 K for 4 h, some samples were quenched to room temperature. The furnace with the remaining samples was cooled at a rate of 5 K min^{-1}. Some samples were removed at 1173, 973 and 773 K and quenched to room temperature. The furnace was then cooled to room temperature at 5 K min^{-1} or at the natural cooling rate, whichever was slower, and the remaining samples were taken out. A set of samples, furnace cooled to room temperature in this manner, was reheated to 1373 K for 4 h and then quenched to room temperature in order to study the reversibility of any changes due to slow cooling. The X-ray diffraction patterns of the various heat-treated samples were almost identical and in agreement with published data.

2.2. *Dielectric measurements*

Sintered samples, after various heat treatments, were polished on two parallel faces and electroded. The temperature dependence of the permittivity and loss tangent was measured in a suitable sample holder in the temperature range 298–898 K, employing an automatic system consisting of a temperature control box (Model 2300, Delta Design, Inc., San Diego, California) and an LCR meter (models 4274A and 4275A, Hewlett Packard, Inc., Palo Alto, California). Sets of measurements were made at 1, 10 and 100 kHz.

2.3 *Raman spectra*

Raman spectra were measured on an Instruments SA Ramanor U-1000 spectrometer using as an excitation source the 514.532 nm line of an Ar^+ ion laser with an output power of 200 mW. The instrument resolution was set at 3 cm^{-1}. The instrument was equipped with a microscope, which gave a focal spot size of the order of a few micrometers. Because of losses within the optical system, only ~10% of the laser power reached the sample surface.

For measuring the temperature dependence of the Raman spectra, the samples were mounted on the cold stage of a MMR Joule–Thomson refrigerator equipped with the MMR K-20 programable temperature controller and capable of cooling from room temperature to 65 K. Thermally conducting grease was used to improve the contact between the cold stage and the sample. The sample thicknesses were set at 0.5 mm to reduce temperature gradients.

2.4. *Neutron diffraction measurements*

Neutron diffraction patterns were recorded at room temperature using the T-1011 diffractometer at the 100 MW Dhruva reactor, Trombay.* The samples were in the form of cylindrical pellets (~11 mm in diameter) and ~20 mm in height). The neutron wavelength was 1.216 Å. The instrument collimations were 0.7/0.5/0.5° from the in-pile to the detector end. The patterns were analyzed by the Rietveld profile refinement technique, using a modified version of the program *DBW*3.2 (Wiles & Young, 1981).

Although earlier work assigned the space group *F*222 (Aurivillius, 1949), *F*2*mm* (Ismailzade, 1960) and *Fmmm* (Li, Wang & Xu, 1985), recent careful X-ray diffraction and group theoretic considerations led Rae, Thompson, Withers & Willis (1990) to confirm $A2_1am$ as the space group for related compounds Bi_3TiNbO_9, $SrBi_2Nb_2O_9$ and $SrBi_2Ta_2O_9$. The $A2_1am$ space group is adopted for $PbBi_2Nb_2O_9$ for the following reason. We have carried out Rietveld refinements using the three space groups *F*222, *F*2*mm* and $A2_1am$, starting from a structural model corresponding to the *Fmmm* structure. The results of refinements carried out with *F*222 were far from satisfactory with anomalous *B* values for several atoms, while *F*2*mm* yielded slightly improved fits compared with *F*222, but still not as good as generally obtained in our laboratory for other ceramic materials. In the case of quenched samples, the final R_p values of 0.0444 with *F*222 and 0.0344 with *F*2*mm* were obtained against 0.0219 obtained with $A2_1am$.

Starting with the structural model indicated in Fig. 1 and the space group $A2_1am$, all possible positional, thermal (*B*) and occupancy (*N*) parameters were refined, in addition to the cell parameters, half-width parameters, zero-angle, scale factor and background parameters. Gaussian peak-shape functions were assumed. The

* The numbered intensity of each measured point on the profile has been deposited with the IUCr (Reference: BR0024). Copies may be obtained through The Managing Editor, International Union of Crystallography, 5 Abbey Square, Chester CH1 2HU, England.

thermal and occupancy parameters were varied separately in the initial cycles to avoid correlations. The occupancy of the Nb site was kept full as a reference. Initially, full occupancies were assumed at the oxygen sites. They were floated in the final stages of refinement and found to remain full. The refined occupancy factors of the cation sites indicated preferential occupancy of Pb^{2+} at the perovskite *A*-sites and Bi^{3+} at bilayer *B*-sites. The total occupancies of Pb and Bi ions over these two sites were in agreement with the nominal stoichiometry within a fraction of their standard deviations. Hence, in the final stages of refinement the combined occupancies of Pb and Bi ions over the *A*- and *B*-sites were constrained to conform to stoichiometry.

The refined atomic positions indicated that the displacements of most of the atoms [except Pb, O(1) and O(4)] from the starting positions coresponding to the average *Fmmm* structure show the same signs as those reported by Thompson *et al.* (1991) for isostructural Bi_3TiNbO_9. However, the signs of the displacements were opposite for three of the parameters *y*(Pb), *x*[O(1)] and *x*[O(4)]. This led to a rather low value of 1.4 for the bond valence of O(1) and a somewhat high value (2.39) for the bond valence of O(4). In order to check the possibility of these three parameters being trapped in false local minima (Thompson, Schmid, Withers, Rae & Fitzgerald, 1992), a further set (II) of refinements was carried out by inverting these three parameters relative to their values in the undistorted structure. These three positions indeed converged around the new (kicked) sites and improved the agreement factors (R_p values) from 0.024 to 0.022 for the quenched samples and from 0.024 to 0.023 for the slow-cooled sample.

Further refinements carried out by inverting the remaining parameters across their values corresponding to the undistorted *Fmmm* structure indicated that most of the parameters revert back to the values obtained in refinement set II, except the three, *x*(Nb), *y*[O(1)] and *y*[O(2)], which converged toward their inverted values, albeit with much poorer agreement factors. Hence, they could not be accepted. The final parameters resulting from the refinement set II, which yielded

Table 1. *Structural parameters from neutron diffraction data*

Parameters		Quenched sample	Annealed sample
Space group		$A2_1am$	$A2_1am$
a (Å)		5.503 (4)	5.504 (3)
b (Å)		5.495 (4)	5.487 (3)
c (Å)		25.531 (5)	25.511 (5)
V (Å^3)		772.0 (8)	770.4 (6)
Pb/Bi	(4*a*)		
x		0.25	0.25
y		0.2695 (27)	0.2693 (27)
z		0.50	0.50
B		2.7 (4)	2.2 (3)
N		0.91/0.09 (7)	0.80/0.20 (7)
Bi/Pb	(8*b*)		
x		0.2655 (72)	0.2662 (54)
y		0.7464 (29)	0.7420 (27)
z		0.2010 (2)	0.2013 (2)
B		0.9 (2)	0.8 (2)
N		0.95/0.05 (7)	0.90.0.10 (7)
Nb	(8*b*)		
x		0.2797 (53)	0.2776 (44)
y		0.7476 (32)	0.7435 (25)
z		0.4114 (2)	0.4115 (2)
B		0.6 (1)	0.2 (1)
N		1.0	1.0
O(1)	(4*a*)		
x		0.3212 (71)	0.3092 (60)
y		0.2048 (64)	0.1936 (46)
z		0.0	0.0
B		2.5 (5)	2.4 (4)
N		1.0	1.0
O(2)	(8*b*)		
x		0.3048 (41)	0.3034 (32)
y		0.2813 (35)	0.2751 (31)
z		0.1592 (2)	0.1593 (2)
B		1.0 (3)	0.2 (2)
N		1.0	1.0
O(3)	(8*b*)		
x		0.5304 (62)	0.5236 (57)
y		0.4976 (21)	0.4977 (23)
z		0.2467 (5)	0.2473 (5)
B		0.8 (2)	0.8 (2)
N		1.0	1.0
O(4)	(8*b*)		
x		0.5243 (57)	0.5283 (41)
y		0.0313 (19)	0.0270 (20)
z		0.5723 (3)	0.5715 (3)
B		0.3 (2)	0.1 (2)
N		1.0	1.0
O(5)	(8*b*)		
x		0.5911 (59)	0.5967 (41)
y		0.5483 (21)	0.5457 (18)
z		0.5833 (3)	0.5846 (3)
B		2.1 (3)	0.8 (3)
N		1.0	1.0

Table 1 (*cont.*)

Parameters	Quenched sample	Annealed sample
Space group	$A2_1am$	$A2_1am$
R factors		
R_p	0.022	0.023
R_{wp}	0.029	0.031
R_{exp}	0.017	0.016
R_{Bragg}	0.004	0.005

The scattering amplitudes (*b* values) used for Bi, Pb, Nb and O were 8.53, 9.40, 7.10 and 5.80 fm, respectively. Figures in parentheses represent the e.s.d.'s referred to the last digit. (100 *N*) represents percentage site occupancy. There was no evidence for preferred orientation and no correction was applied. Other data: monochromator (002) pyrolytic graphite; absorption = 0.0093 cm^{-1}; no correction applied. Scan range = 4.70–74.7° 2θ; step size = 0.1° 2θ. No regions of the pattern were omitted. Weights used in refinement $wi = 1/N_i$; Ni = counts at *i*th step. $(\Delta/\sigma)_{max}$ for final cycle = 0.013. The molecular weight for the compound = 954.96, giving a calculated density of 8.214 g cm^{-3} for the quenched sample and 8.231 g cm^{-3} for the slow cooled sample.

Table 2. *Bond distances (Å) and angles (°) for* $PbBi_2Nb_2O_9$

	Quenched sample	Annealed sample
Pb—O(1^{i})	2.364 (39)	2.351 (29)
Pb—O(1^{ii})	2.424 (38)	2.435 (33)
Pb—O(1^{iii})	3.128 (38)	3.085 (33)
Pb—O(1^{iv})	3.147 (39)	3.176 (29)
Pb—O($4^{v,vi}$)	2.720 (20) × 2	2.728 (16) × 2
Pb—O($4^{vii,viii}$)	2.772 (18) × 2	2.731 (15) × 2
Pb—O($5^{ix,x}$)	2.508 (15) × 2	2.530 (12) × 2
Pb—O($5^{v,vi}$)	3.224 (21) × 2	3.256 (16) × 2
Bi—O(2^{x})	2.755 (42)	2.765 (32)
Bi—O(2^{v})	2.778 (24)	2.784 (21)
Bi—O(2^{xi})	3.134 (24)	3.122 (22)
Bi—O(2^{xii})	3.157 (43)	3.147 (33)
Bi—O(3^{x})	2.198 (34)	2.211 (29)
Bi—O(3^{v})	2.314 (36)	2.276 (30)
Bi—O(3^{xiii})	2.331 (32)	2.354 (28)
Bi—O(3^{xiv})	2.411 (34)	2.386 (29)
Nb—O(1^{ii})	2.286 (8)	2.281 (7)
Nb—O(2^{xiv})	1.817 (8)	1.820 (8)
Nb—O(4^{xv})	1.904 (34)	1.913 (26)
Nb—O(4^{xvi})	2.101 (31)	2.124 (25)
Nb—O(5^{ix})	1.934 (29)	1.876 (23)
Nb—O(5^{vi})	2.038 (38)	2.067 (30)
O(1^{ii})—Nb—O(2^{xiv})	170 (2)	171 (2)
O(1^{ii})—Nb—O(4^{xv})	86 (1)	85 (1)
O(1^{ii})—Nb—O(4^{xvi})	79 (1)	81 (1)
O(1^{ii})—Nb—O(5^{ix})	84 (1)	83 (1)
O(1^{ii})—Nb—O(5^{vi})	78 (1)	81 (1)
O(2^{xiv})—Nb—O(4^{xv})	102 (1)	103 (1)
O(2^{xiv})—Nb—O(5^{ix})	101 (1)	100 (1)
O(2^{xiv})—Nb—O(4^{xvi})	94 (1)	95 (1)
O(2^{xiv})—Nb—O(5^{vi})	93 (1)	92 (1)
O(4^{xv})—Nb—O(4^{xvi})	87 (1)	86 (1)
O(4^{xv})—Nb—O(5^{ix})	97 (2)	99 (2)
O(4^{xv})—Nb—O(5^{vi})	162 (1)	161 (1)
O(5^{ix})—Nb—O(4^{xvi})	163 (1)	162 (1)
O(5^{ix})—Nb—O(5^{vi})	90 (1)	90 (1)
O(5^{vi})—Nb—O(4^{xvi})	81 (1)	80 (1)
Nb^{xvii}—O(1)—Nb^{xviii}	164 (2)	164 (2)

Symmetry codes: (i) $x-\frac{1}{2}, \frac{1}{2}-y, \frac{1}{2}-z$; (ii) $x, \frac{1}{2}+y, \frac{1}{2}+z$; (iii) $x, y-\frac{1}{2}, \frac{1}{2}+z$; (iv) $\frac{1}{2}+x, \frac{1}{2}-y, \frac{1}{2}-z$; (v) x, y, z; (vi) $x, y, 1-z$; (vii) $x-\frac{1}{2}, -y, 1-z$; (viii) $x-\frac{1}{2}, -y, z$; (ix) $x-\frac{1}{2}, 1-y, 1-z$; (x) $x-\frac{1}{2}, 1-y, z$; (xi) $x, 1+y, z$; (xii) $\frac{1}{2}+x, 1-y, z$; (xiii) $x-\frac{1}{2}, \frac{3}{2}-y, \frac{1}{2}-z$; (xiv) $x, \frac{1}{2}+y, \frac{1}{2}-z$; (xv) $x-\frac{1}{2}, 1-y, 1-z$; (xvi) $x, 1+y, 1-z$; (xvii) $x, y-\frac{1}{2}, z-\frac{1}{2}$; (xviii) $x, y-\frac{1}{2}, \frac{1}{2}-z$.

the best agreement factors, are listed in Table 1 and the corresponding interatomic distances and angles are given in Table 2. The calculated bond valence sums associated with the different cation and anion sites are given in Table 3. The low and high sums for O_2 and O_3, respectively, are in agreement with other $n = 2$ members of the Aurivillius family (*e.g.* Bi_3TiNbO_9). The valence sums for the Pb and Bi sites are similar in quenched and annealed samples and average 2.56 for the Pb site and 2.7 for the Bi site. This indicates cation disorder of similar magnitude in both samples and thus does not provide unambiguous support for a change in disorder with heat treatment temperatures. It may be noted that significantly higher values of bond valence sums for

Table 3. *Bond valence sums (v.u.) for* $PbBi_2Nb_2O_9$

Site	Quenched	Annealed
Pb	2.57	2.56
Bi	2.70	2.73
Nb	4.92	4.96
O(1)	1.79	1.81
O(2)	1.73	1.72
O(3)	2.26	2.29
O(4)	1.98	1.93
O(5)	2.04	2.12
R_1	0.27	0.27

$V = \sum \exp(r_o - r_j)/0.37$ with parameters of $r_o = 2.112$ (Pb), 2.094 (Bi), 1.911 (Nb). Parameters from Brown & Altermatt (1985). R_1 is the goodness-of-fit parameter.

A-sites and lower values for *B*-sites have also been reported for isostructural $SrBi_2Ta_2O_9$ and attributed to overbonding of the divalent cation occupying the perovskite *A*-site (Rae *et al.*, 1992). Distortion from the high-symmetry parent structure is expected to cause overbonding of the *A*-site atoms and underbonding of Bi on the *B*-site. Our results are also in line with the observations of Rae *et al.* (1992).

3. Results

3.1. *Dielectric studies*

The temperature dependence of the permittivity of $PbBi_2Nb_2O_9$ samples after a variety of heat treatments is shown in Fig. 2. The ferroelectric Curie temperature (T_c) was found to decrease with the decrease in the temperature from which the sample was quenched (Fig. 3). The highest T_c, 883 K, was displayed by the sample quenched from the highest temperature, 1373 K, and the lowest T_c, 833 K, by the sample slow-cooled in the furnace from 1373 to 773 K. The fact that the sample

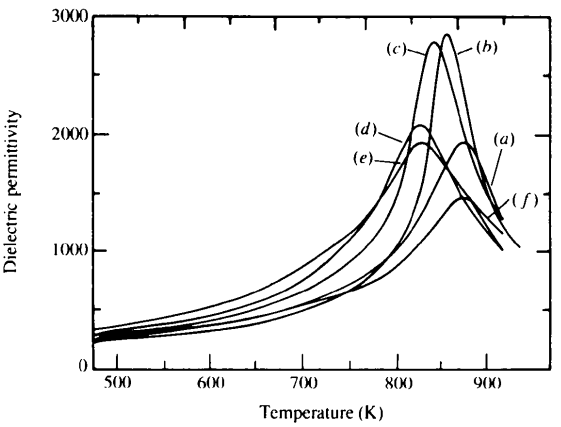

Fig. 2. Temperature dependence of the dielectric permittivity of $PbBi_2Nb_2O_9$. (*a*) Ceramic quenched from 1373, (*b*) 1173, (*c*) 973, (*d*) 773 K, (*e*) furnace-cooled from 1373 K at 5 K min^{-1} and (*f*) originally furnace-cooled then reheated to 1373 K for 4 h and quenched.

which was furnace-cooled to 773 K at 5 K min^{-1} and then quenched (*D*) has almost the same T_c as the sample cooled to temperatures below 773 K at 5 K min^{-1} (*E*) suggests that no structural rearrangements occur below 773 K on the timescale of these experiments. A furnace-cooled sample on reheating to 1373 K and then quenched (*F*) exhibits an enhanced T_c, similar to sample *A*. This indicates that the shift of T_c can be fully reversed by the appropriate heat treatment.

The effect of annealing time on T_c and accompanying structural rearrangements of $PbBi_2Nb_2O_9$ was investigated by quenching samples after 1, 10, 100 and 240 min. T_c shifts to higher temperature with increasing annealing time and reaches an equilibrium value. The equilibrium T_c is reached faster (about 10 min) at 1373 K than at 973 K (10–100 min), as may be expected for a diffusion-controlled process.

The dielectric data at 1, 10 and 100 kHz on $PbBi_2Nb_2O_9$ samples quenched from 1373 K and from 773 K after cooling from 1373 to 773 K at the rate 5 K min^{-1} are shown in Fig. 4. The permittivity peak occurs at the same temperature for all three frequencies in each case, suggesting the absence of relaxor-type behavior in $PbBi_2Nb_2O_9$, irrespective of the heat treatment. This differs from the reported relaxor-type behavior in $BaBi_2Nb_2O_9$ (Newnham *et al.*, 1971). However, the peak in the permittivity–temperature plot is broader for the furnace-cooled sample compared with the sample quenched from 1373 K.

3.2. *Raman studies*

Raman spectra of $PbBi_2Nb_2O_9$ samples quenched from various temperatures in the range 773–1373 K and also those cooled in the furnace were measured at room temperature (295 K) and 80 K (Fig. 5). At room temperature the spectra of the quenched and annealed samples are identical to within limits of measurement. When the samples are cooled to 80 K, all Raman bands sharpen and there is some improved resolution as is characteristic of this class of compounds, although the magnitude of the effect is much less than for the structurally similar $Bi_4Ti_3O_{12}$ (Idink, Srikanth, White & Subbarao, 1994). The spectral features of quenched and annealed samples above 100 cm^{-1} at 80 K are very similar. However, a distinctly different pattern of bands occurs in the low wavenumber range between 20 and 100 cm^{-1}. This region was examined in detail.

The wavenumbers of selected Raman bands in the range 10–100 cm^{-1} are plotted as a function of quenching temperature for spectra taken at 295 and 80 K in Fig. 6. The full widths at half maximum for these Raman bands are plotted in Fig. 7. Most of the bands in the low wavenumber region are weak and some, the *L* and *N* bands, appear only as shoulders on the more intense 63 cm^{-1} *M* band. The wavenumber shift of the Raman modes is independent of the quenching temperature for the spectra taken at 295 K (Fig. 6*a*). All bands which appeared in the 295 K spectra shift slightly to higher wavenumbers in the 80 K spectra. The band width of the *L* band decreases from 20 cm^{-1} at 295 K to 10 cm^{-1} at 80 K, whereas the widths of the other bands decrease only slightly with temperature.

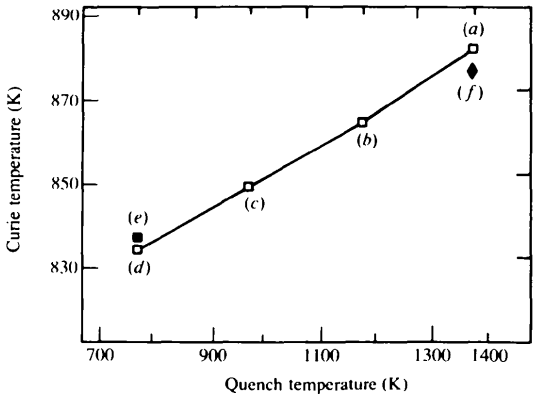

Fig. 3. Variation of Curie temperature as a function of quenching temperature. The sample designations are as defined in Fig. 2.

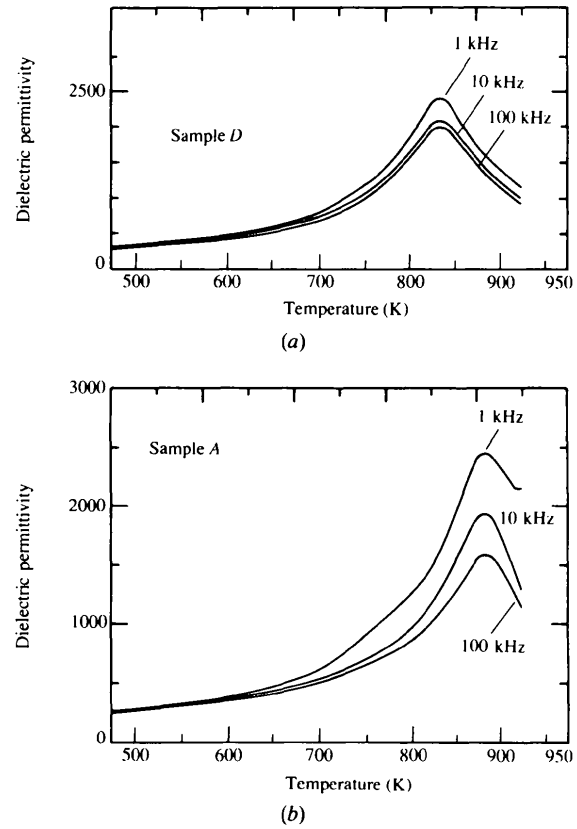

Fig. 4. Temperature dependence of dielectric permittivity of $PbBi_2Nb_2O_9$ at 1, 10 and 100 kHz for (*a*) quenched from 1373 K and (*b*) furnace-cooled to 773 K.

The most interesting feature in the spectra at 80 K is an additional intense band, the *P* band, which appears at 49–51 cm^{-1} in all the quenched samples but which is absent in the spectra of the annealed sample (Fig. 6*b*). The half width of the *P* band is strongly dependent on the quenching temperature, with larger values for samples quenched from 973 to 1173 K compared with those quenched from 1373 K (Fig. 7).

3.3. *Neutron diffraction studies*

The neutron diffraction data on powder samples of two $PbBi_2Nb_2O_9$ samples, one quenched from 1373 K and the other furnace-cooled from 1373 K at the rate 5 K min^{-1}, were utilized to obtain lattice parameters (Table 1) employing Rietveld refinement (Fig. 8). In the orthorhombic $A2_1am$ space group there are two equipoint positions: general and mirror plane sites. The general position 8(*b*) consists of x,y,z; $x,y+\frac{1}{2},z+\frac{1}{2}$; $x,y,-z$; $x,y+\frac{1}{2},\frac{1}{2}-z$; $\frac{1}{2}+x,-y,-z$; $\frac{1}{2}+x,\frac{1}{2}-y,\frac{1}{2}-z$; $\frac{1}{2}+x,-y,z$; $\frac{1}{2}+x,\frac{1}{2}-y,\frac{1}{2}+z$. The mirror plane 4(*a*) positions contain $x,y,0$; $x,\frac{1}{2}+y,\frac{1}{2}$; $\frac{1}{2}+x,-y,0$; $\frac{1}{2}+x,\frac{1}{2}-y,\frac{1}{2}$. In $PbBi_2Nb_2O_9$ all atoms are in general positions, except Pb and O(1). The differences between the two samples are small. Despite the poor contrast between the scattering amplitudes of Bi (8.53) and Pb (9.40), the refined occupancy factors do indicate the presence of order–disorder involving the Pb and Bi sites, with the Pb^{2+} ions occupying the perovskite sites to the extent of 91 (7) and 80 (7)% in the quenched and the slow-cooled samples, respectively. The cell parameters reflect the presence of small amounts of compressive strain and marginally larger orthorhombicity in the furnace-cooled sample relative to the quenched one.

4. Discussion

In the crystal structure of $A^{2+}Bi_2{}^{3+}Me_2{}^{5+}O_9$ compounds of the Aurivillius type, where A^{2+} is a large divalent cation such as Pb^{2+}, Ba^{2+} or Sr^{2+} and Me^{5+} is an intermediate size pentavalent ion such as Nb^{5+} or Ta^{5+}, Bi^{3+}

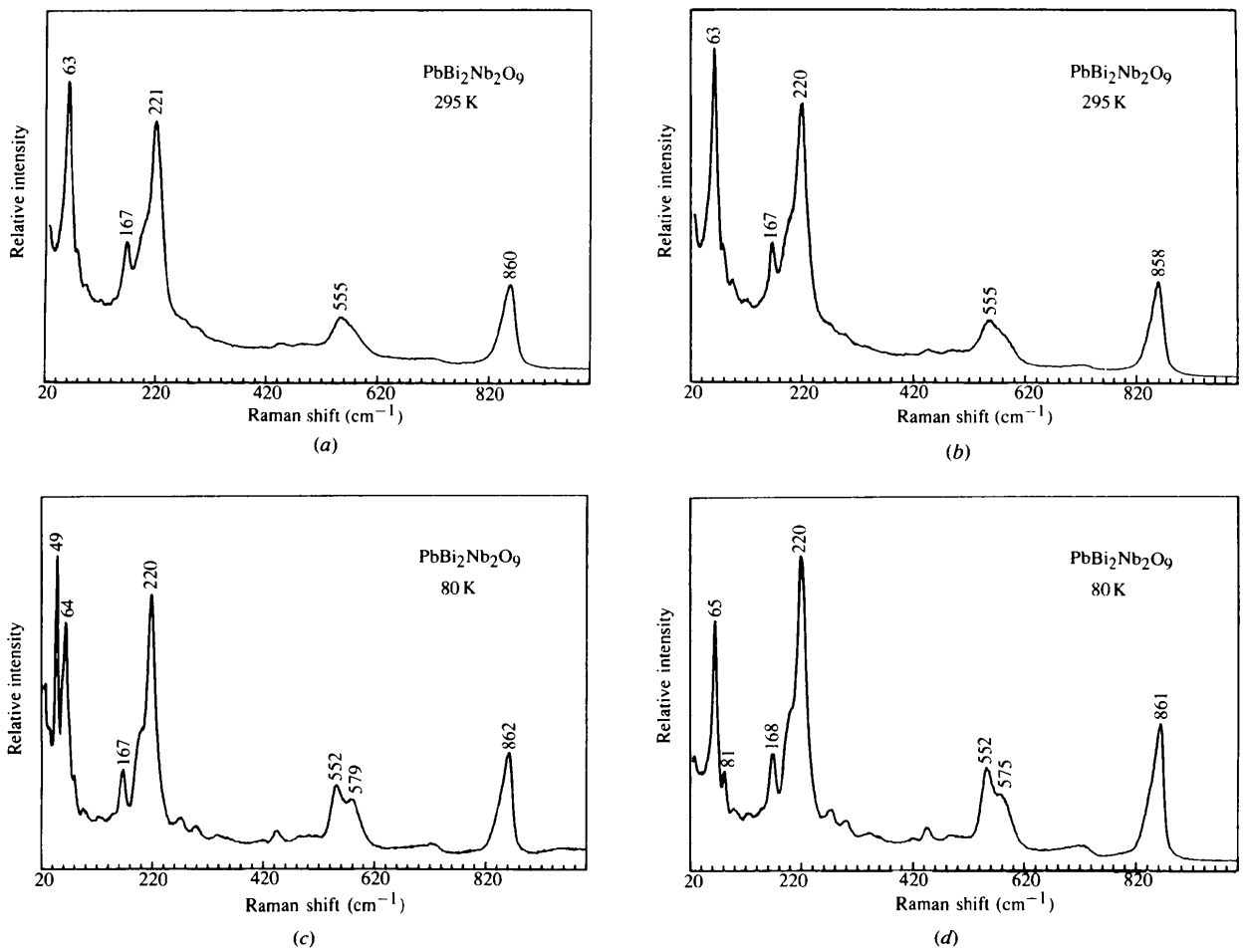

Fig. 5. Raman spectra of $PbBi_2Nb_2O_9$, quenched from 1373 K (*a* and *c*) and cooled in the furnace from 1373 K at 5 K min^{-1} (*b* and *d*). (*a*) and (*b*) are obtained at 295 K and (*c*) and (*d*) at 80 K.

ions occupy the cation sites in the Bi_2O_2 layer, while the A^{2+} ions occupy the large site of the $AMeO_3$ perovskite units. However, in a related compound Bi_3TiNbO_9 and also in $Bi_4Ti_3O_{12}$ (Aurivillius, 1949, 1950, 1952) the cation sites in the Bi_2O_2 layers as well as the *A*-sites of the perovskite units are occupied by Bi^{3+} ions. Thus, Bi^{3+} can, in principle, occupy the *A*-sites of the perovskite units in the Aurivillius phases. Due to the similarity of the ionic size and electronic configuration of Pb^{2+} and Bi^{3+} ions, it appears plausible that Pb^{2+} and Bi^{3+} ions interdiffuse between the two types of cation sites. The extent of such interdiffusion depends on the heat treatment and the annealing temperatures. Slightly larger proportions of Pb^{2+} ions seem to be present in the perovskite units in samples quenched from higher temperatures than in those quenched from successively lower temperatures. Similarly, the interdiffusion continues with time at a given temperature until an equilibrium cation distribution is attained. In this connection it is interesting to note that Millan, Castro & Torrance, (1993) have been able to completely substitute Bi^{3+} in the Bi_2O_2 layer of a related compound, $SrBi_2Nb_2O_9$, by Pb^{2+} accompanied by oxygen vacancies.

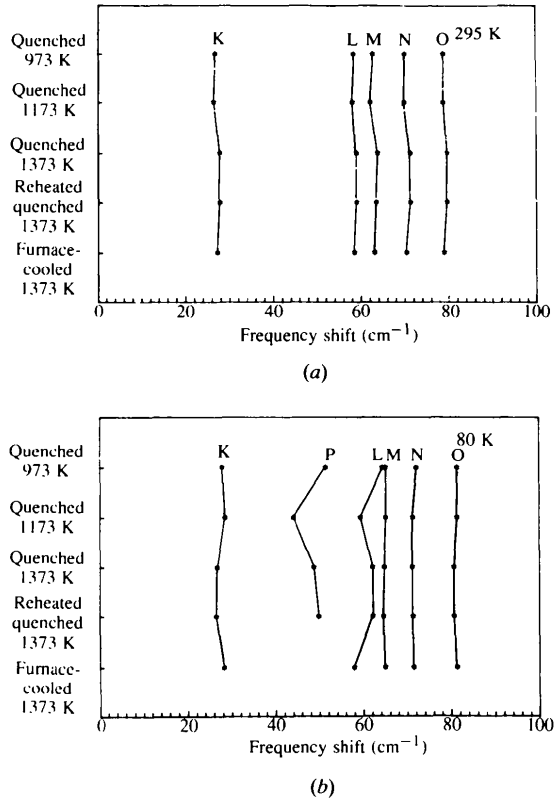

Fig. 6. Wavenumber shift of low wavenumber Raman bands as a function of quenching temperature for spectra collected at 295 and 80 K.

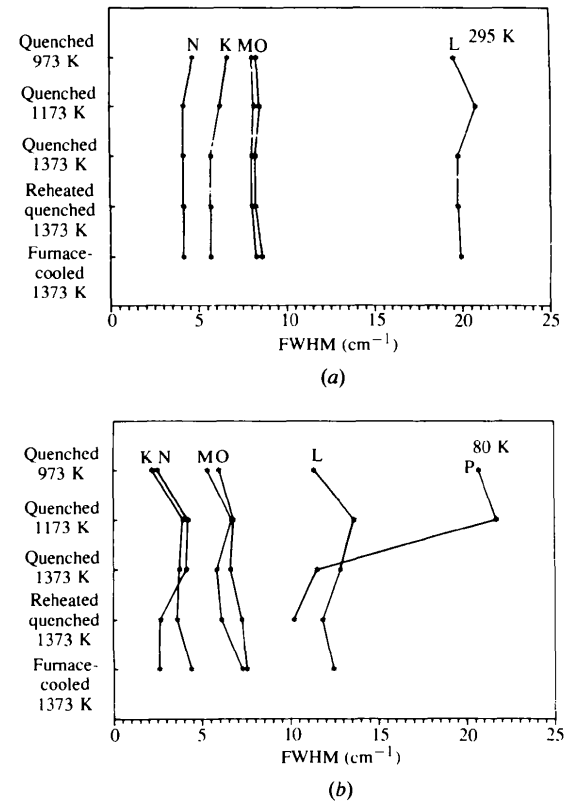

Fig. 7. Full width at half maximum (FWHM) of selected Raman bands of $PbBi_2Nb_2O_9$ as a function of quenching temperature for spectra collected at 295 and 80 K.

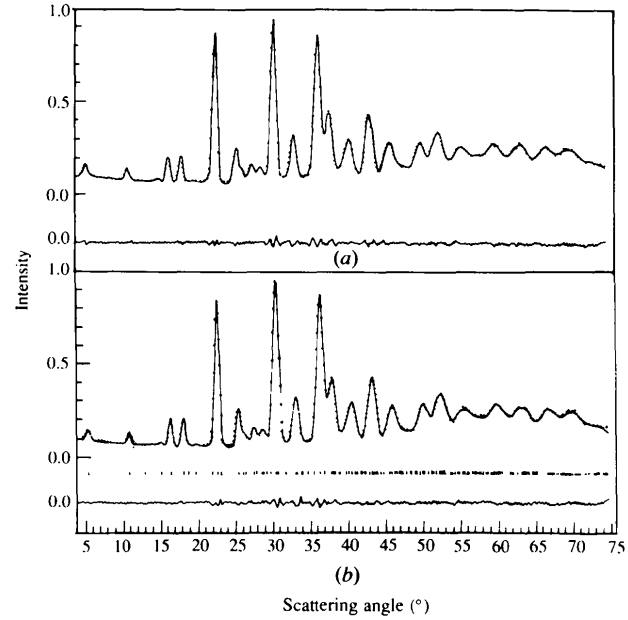

Fig. 8. Observed and Rietveld fitted neutron diffraction patterns for $PbBi_2Nb_2O_9$: (*a*) quenched and (*b*) furnace-cooled.

From the neutron diffraction data, the sample quenched from 1373 K apppears slightly more ordered than that which was furnace-cooled. The $PbBi_2Nb_2O_9$ samples quenched from higher temperatures exhibit higher T_c values compared with the T_c values of samples quenched from lower temperatures which possess cation disorder (Figs. 2 and 3). The reversibility of the shift of T_c with the appropriate heat treatment is also consistent with this proposition. The increase in T_c with annealing time up to a certain equilibrium T_c for a given quenching temperature and the attainment of the equilibrium T_c in a shorter time for higher quenching temperatures is also supportive of the cation interdiffusion model. The broader peaks for the disordered materials in the dielectric permittivity–temperature plots are as expected (Fig. 4).

The low-temperature Raman spectra provide strong evidence for differing structures in the various quenched and annealed samples. The *P* band, at 51 cm^{-1}, appears in the 80 K spectra of the quenched samples, but not in the spectrum of the annealed sample. This sharp intense band does not appear at all in the 295 K spectra. It is significant that the width of the *P* band exhibits strong dependence on the quenching temperature (Fig. 7). The *P* band line width is broad for samples quenched from 973 and 1173 K. The line width sharply decreases for samples quenched from 1373 K.

As an isolated feature, the *P* band cannot be assigned to a specific atomic motion. Low-wavenumber Raman lines arise from bond stretching motions of heavy high coordination number cations such as Pb^{2+} and Bi^{3+} and from cooperative movements of the entire unit cell. Order/disorder effects or phase transitions cause new bands or substantial changes in line width in this wavenumber range. There may be little or no change in the high wavenumber bands, which are more related to the nearest-neighbor structural relations. The low-wavenumber Raman spectra show quite clearly the effects of differing heat treatments, but do not permit their interpretation in specific structural terms.

5. Conclusions

The similarity of size and electronic configuration of Pb^{2+} and Bi^{3+} ions make plausible the interdiffusion of the two ions between the cation sites in the Bi_2O_2 layer and the *A*-sites of the perovskite unit in the crystal structure of $PbBi_2Nb_2O_9$. The disorder and the concomitant structural distortion (orthorhombicity) is minimum in samples quenched from highest temperatures or after sufficiently long annealing at lower temperatures. The degree of cation disorder correlates with the ferroelectric Curie temperature of $PbBi_2Nb_2O_9$. These effects are reversible. Low-wavenumber Raman spectra also show structural sensitivity of heat treatment of the compounds.

This work was supported by the Office of Naval Research.

References

Aurivillius, B. (1949). *Arkiv. Kemi*, **1**, 463–480, 499–512.
Aurivillius, B. (1950). *Arkiv. Kemi*, **2**, 519–527.
Aurivillius, B. (1952). *Arkiv. Kemi*, **5**, 39–47.
Brown, I. D. & Altermatt, D. (1985). *Acta Cryst.* B**41**, 244–247.
Graves, P. R., Hua, G., Myhra, S. & Thompson, J. G. (1995). *J. Solid State Chem.* **114**, 112–122.
Idink, H., Srikanth, V., White, W. B. & Subbarao, E. C. (1994) *J. Appl. Phys.* **76**, 1789–1793.
Ismailzade, I. G. (1960). *Izv. Akad. Nauk SSSR, Ser. Fiz.* **24**, 1198–1202.
Li, D.-Y., Wang, P.-L. & Xu, Y.-Y. (1985). *Acta Phys. Sin.* **34**, 946–950.
Millan, P., Castro, A. & Torrance, J. B. (1993). *Mater. Res. Bull.* **28**, 117–122.
Newnham, R. E., Wolfe, R. W. & Dorrian, J. F. (1971). *Mater. Res. Bull.* **6**, 1029–1040.
Newnham, R. E., Wolfe, R. W., Horsey, R. S., Diaz-Colon, F. A. & Kay, M. I. (1973). *Mater. Res. Bull.* **8**, 1183–1196.
Rae, A. D., Thompson, J. G. & Withers, R. L. (1992). *Acta Cryst.* B**48**, 418–428.
Rae, A. D., Thompson, J. G., Withers, R. L. & Willis, A. C. (1990). *Acta Cryst.* B**46**, 474–487.
Smolenskii, G. A., Isupov, V. A. & Agranoskaya, A. I. (1961). *Sov. Phys. Solid State*, **3**, 651–655.
Subbarao, E. C. (1962*a*). *J. Phys. Chem. Solids*, **23**, 665–676.
Subbarao, E. C. (1962*b*). *J. Am. Ceram. Soc.* **45**, 166–169.
Thompson, J. G., Rae, A. D., Withers, R. L. & Craig, D. C. (1991). *Acta Cryst.* B**47**, 174–180.
Thompson, J. G., Schmid, S., Withers, R. L., Rae, A. D. & Fitzgerald, J. D. (1992). *J. Solid State Chem.* **101**, 309–321.
Wiles, D. B. & Young, R. A. (1981). *J. Appl. Cryst.* **14**, 149–151.
Wolfe, R. W., Newnham, R. E., Smith, D. K. & Kay, M. I. (1971). *Ferroelectrics*, **3**, 1–7.